ELSEVIER

Carbohydrate Research 292 (1996) 21–38

CARBOHYDRATE RESEARCH

The hydration of sucrose

Søren B. Engelsen [a], Serge Pérez [b,*]

[a] *The Royal Veterinary and Agricultural University, Department of Dairy and Food Science, Food Technology, Rolighedsvej 30, DK-1958 Frederiksberg C, Denmark*

[b] *Centre de Recherches sur les Macromolécules Végétales [1], CNRS, BP 53X, 38041 Grenoble Cédex, France*

Received 3 April 1996; accepted 12 July 1996

Abstract

The structural and dynamical features of the hydration of sucrose have been derived from a 500 ps molecular dynamics simulation with explicit water molecules. In order to obtain the degree and structure of the solvation of the sucrose solute, radial atomic pair distribution functions have been calculated between selected solute atoms and the water molecules. The analysis provides a molecular hydration number of 37.6 water molecules in the first hydration shell. If the 'hydration criterion' is restricted to include oxygen–oxygen distances less than 2.8 Å, an average hydration number of 7 is obtained, which is close to that derived experimentally from viscosity and apparent molar volume. This indicates that the firmly hydrogen bonded water molecules have more impact on the macroscopic properties than the shielding effect formed by the first hydration shell. Both the radial and orientational hydration of acetal and hydroxyl oxygens have been fully characterized. The analysis reveals significant differences between the glycosidic oxygen and the ring oxygen atoms. It also shows that the water structure around the three secondary hydroxyl groups of the pyranosyl moiety is more structured than around the rest of the molecule. This indicates a more perfect hydration of this relatively rigid part of sucrose. The residence times for polar water molecules around the sucrose solute were also characterized. Whereas typical values are in the order of 1 to 2 ps, some extremely long residence times of about 30 ps may occur in the vicinity of the O-3 hydroxyl group of the fructofuranosyl moiety. Extension of the analysis to significant bridging water molecules points towards the existence of two cases (O-2g...Ow...O-3f and O-2g...Ow...O-1f) being populated more than 41% and 66% of the time. In comparison, the direct interresidue hydrogen bond O-2g...O-1f is populated less than 4% of the time. The bridging water between O-2g and O-3f is found in the crystalline complex between sucrose and a lentil lectin. In an aqueous environment the ability of sucrose to establish these water-mediated hydrogen bonds between its two moieties may be relevant in explaining the oversaturation range

* Corresponding author.

[1] Affiliated with the Université Joseph Fourier at Grenoble.

PII S0008-6215(96)00184-X

which prevails before nucleation occurs. It may also have significant implications as far as the sweet-taste elicitation mechanism is concerned. © 1996 Elsevier Science Ltd.

Keywords: Sucrose; Hydration; Molecular dynamics; Protein/carbohydrate

1. Introduction

With eight hydroxyl groups, three hydrophilic oxygen atoms, and fourteen hydrogen atoms, the sucrose molecule can readily interact through hydrogen bonding with water, molecules, and proteins. Characterizing the structural features of hydration of sucrose at the molecular level is of fundamental importance in understanding such points as (1) the dissolution and supersaturation behaviour, (2) the driving force of crystal growth, (3) the reactivity, (4) transport into receptor epithelium, and (5) sweet taste reception.

The conformation of sucrose in aqueous solution has been the subject of many investigations, the results of which have been somewhat controversial. Actually, it may be difficult to extract an unequivocal picture, as sucrose conformational behaviour is likely to be concentration dependent. Nevertheless, the body of experimental observations indicates that two intra-molecular hydrogen bonds exist in the crystalline state, and possibly at high concentration, but they are successively broken upon dilution, with a single hydrogen bond persisting at intermediate concentration (see review [1] and references therein).

It is only recently that the first pictures, at the atomic level, could be obtained for the hydration of sucrose. The first picture was provided by a 1 ns molecular dynamics simulation of an aqueous solution of sucrose [2]. The radius of gyration, overall molecular tumbling time, and self-diffusion coefficient of sucrose in aqueous solution were established from the molecular dynamic simulation; they compared extremely well with the corresponding experimental values. Equally satisfactory was the good agreement obtained for such NMR observables as the glycosidic heteronuclear coupling constants and high resolution NMR relaxation data. Among many features, it was shown that neither of the two crystallographic intramolecular hydrogen bonds (O-2g...HO-1f and O-5g...HO-6f) persist durably in aqueous solution. This has later and independently been confirmed [3], as evidence of a low populated transient O-2g...O-1f interresidue hydrogen bond in supercooled solution using high resolution ROESY experiments was found. Finally, of particular interest was the observation of a 25% populated water bridging conformation: O-2g...Ow...O3-f in the molecular dynamics trajectories.

The second picture was provided by the crystallographic investigation of the first complex between sucrose and a protein, lentil lectin, at 1.9 Å resolution [4]. Two hundred and twenty-eight water molecules were located, some in close interaction with the sucrose molecules. No detailed description of the hydration scheme was attempted in either of these two studies. It is the aim of the present study to investigate the wealth of structural information provided by the molecular dynamics simulation as well as the crystalline structure in order to assess the molecular features of the hydration of sucrose in addition to their chemical and biological implications.

2. Methods

Nomenclature.—A schematic heavy atom representation of sucrose (β-D-fructofuranose-(2-1)-α-D-glucopyranoside) with its eight hydroxyl and three acetal oxygens is shown in Fig. 1. Conformational flexibility around the glycosidic linkage bonds is described by the two torsional angles: Φ = O-5g–C-1g–O-1g–C-2f and Ψ = C-1g–O-1g–C-2f–O-5f and the conformations of the three hydroxymethyl groups are described by the torsional angles: ω_g = O-5g–C-5g–C-6g–O-6g, ω_f = O-5f–C-5f–C-6f–O-6f, and χ_f = O-5f–C-2f–C-1f–O-1f. The three staggered orientations of the primary hydroxyl groups are also referred to as either *gauche–gauche* (GG), *gauche–trans* (GT) or *trans–gauche* (TG), depending on whether the values of the above torsion angles are closest to 60°, 60° or 180°, respectively. The sign of the torsion angles is defined in agreement with the IUPAC Commission of Biochemical Nomenclature [5]. Another parameter of interest is the magnitude of the valence angle at the glycosidic linkage: C-1g–O-1g–C-2f.

Throughout this paper the Cremer–Pople convention is used [6] where pseudo-rotational parameters q_2 and ϕ_2 describe the ring conformation of the flexible fructofuranosyl residue which can be related to one of the twenty different twist (T) and envelope (E). Their description involves an amplitude which measures the deviation from planarity, and a phase angle that describes the type of distortion.

Molecular dynamics simulation.—Since the details of the molecular dynamics (MD) simulation have been described elsewhere [2], only those essential to the understanding

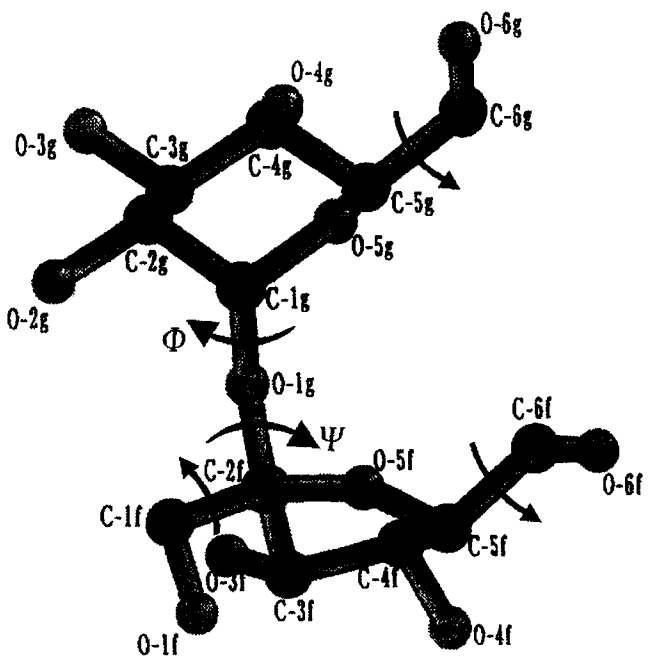

Fig. 1. Heavy atom representation of sucrose including atomic labels.

of the present study are presented. The solution behaviour of sucrose was investigated by calculating a total ensemble of 1.2 ns MD trajectories from an ensemble of five micro-canonical trajectories. This was performed using the carbohydrate force field [7] implemented in the general molecular mechanics CHARMm program [8]. The water molecules of the solvent were modelled using the TIP3P potential energy function [9]. In the simulation, Newton's equations of motion were integrated for each atom using the two-step velocity Verlet algorithm [10]. All hydrogen atoms were explicitly included in the simulations, although bond lengths involving hydrogen atoms were kept fixed throughout the simulation using the constraint algorithm SHAKE [11]. The explicit water phase was mimicked in the form of 512 water molecules captured in a cubic box using minimum image boundary conditions. Interactions between atoms more than 12 Å apart were truncated, and switching functions were used to smoothly turn off long range interactions between 10 and 11 Å.

In this study we analyze the hydration of sucrose from the 500 ps trajectory which corresponds to one micro-canonical trajectory where the initial coordinates of the solute were taken as the crystalline structure [12]. The coordinates of the crystal conformation of sucrose were superimposed upon the coordinates of a well equilibrated box of water which left 489 water molecules in the primary box. Then the cubic box length was slightly adjusted to give the experimental density for the actual concentration of 3.74% (w/w). The initial velocity for all atoms was assigned from a Boltzmann distribution at 300 K. The system was equilibrated for 20 ps to relax any artificial starting conditions. Following the equilibration period, the integration was continued without further interference. Complete phase points were saved every 0.02 ps for subsequent analysis.

Analysis of water structure.—Radial pair distribution functions. In order to obtain the degree and structure of the solvation of the sucrose solute, radial atomic pair distribution functions $g(r)$ are calculated between selected solute atoms and the water molecules. The radial pair distribution function is expressed by the formula [13]:

$$g(r) = \frac{1}{4\pi\rho_w r^2} \frac{dN(r)}{dr}$$

where r is the interatomic distance between the solute atom and the water molecules, ρ_w is the bulk water number density and $N(r)$ is the average number of solvent molecules (water oxygens) at a distance between r and $r + dr$ from the solute atom. $g(r) \times dr$ is the probability of finding a water molecule (oxygen) in the range r to $r + dr$ from the solute atom. In liquids with short range order, pair distributions will often display oscillating behaviour with decreasing magnitude. This shell type liquid structure induced by the solute and decreasing in order with the distance to the solute is due to optimal arrangements of solvent hydrogen bonds. The first sphere of nearest neighbours is indicated by a peak in $g(r)$ and limited by a minimum in $g(r)$ and is referred to as the first hydration shell. While the coordination number of the solute oxygens can be readily obtained from the maximum $g(r)$, the average number of close neighbours in the first hydration shell around the solute oxygens is obtained by integration of the radial pair distribution functions to a given radius from the solute atoms.

Orientational distribution functions for water molecules. In order to analyze the orientational behaviour of polar water molecules, orientational distribution functions,

$p(\cos(\theta))$, for water molecules within 3.5 Å from selected solute oxygen atoms were calculated. This was done by calculating the two angles θ(Ow–H1...O_s) and θ(Ow–H2...O_s) for all water molecules within a given distance (3.5 Å) from the solute oxygen O_s (or alternatively a solute carbon C_s). The normalized distribution was plotted versus the cosine to the angles. Such orientational distribution functions often display a dual peak behaviour with a secondary peak caused by the tetrahedral geometry of the rigid TIP3P water molecules. For comparison with the hydration found in a crystal structure where only the heavy atoms are located, a similar type of orientational distribution function was calculated for the angles θ(Cs–Os...Ow) around all the hydroxyl solute oxygens.

Residence times etc. Maximum and average residence times for polar water molecules as well as total hydration number, h, of the sucrose solute are calculated using programs specifically written in FORTRAN for analyzing the trajectory on a frame by frame basis.

Crystal structure of sucrose complexed to lentil lectin.—The sucrose–lentil lectin complex [4] crystallizes in the monoclinic $P2_1$ space group. The unit cell having parameters: $a = 50.03$ Å, $b = 124.0$ Å, $c = 50.02$ Å, $\beta = 111.80°$ contains a complete lectin dimer in the asymmetric unit. X-ray data were collected to a resolution of 1.9 Å, and the structure was refined to an R value of 18.8%. Completion of the structure provided location of all the atoms in the protein dimer, 228 solvent atoms (water oxygens), 2 Mn^{2+}, 2 Ca^{2+}, and two crystallographically independent sucrose molecules. From the atomic coordinates which have been deposited in the Protein Data Bank at the Brookhaven National Laboratory [14] with the code 1LES, all the structural features required to assess the hydration of sucrose in such a neighbourhood can be computed.

The hydration of the two sucrose molecules in the lectin complex is shown in Fig. 2 which shows the proximity of the two sucrose molecules in the lectin dimer. Details of

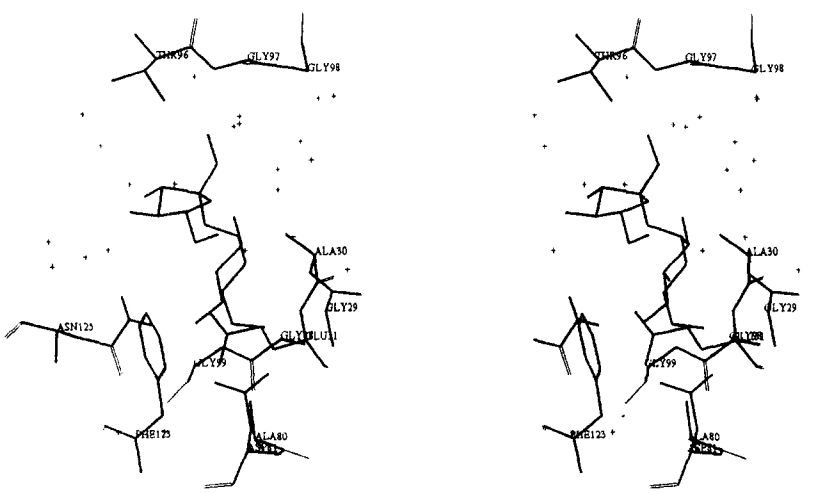

Fig. 2. Stereo view of the hydration of sucrose complexed to the lentil lectin at a 1.9 Å resolution. As the sucrose–lentil lectin complex crystallizes as dimer, two crystallographically independent sucrose molecules are found. However, since the sucrose molecules and their surroundings are very similar, only one has been represented.

Table 1
The sucrose hydration as found in the lectin crystal [4]. Distances are in Å and angles are in deg

Conformation	X-ray	L1	L2
Φ	107.8°	105°	104°
Ψ	−44.8°	−57°	−58°
θ	114.3°	118°	118°
ω_g	−56.4°	−37°	−36°
ω_f	−69.6°	80°	77°
χ_f	171.4°	−47°	−68°
q_2	0.353	0.462	0.465
ϕ_2	265.2°	258.9°	259.7°
O-2g...O-1f	2.78	4.90	4.93
O-2g...O-3f	4.84	4.45	4.51
O-5g...O-6f	2.85	4.48	4.50
Ow1...O-2g(–C-2g)		2.75 (120°)	2.80 (127°)
Ow1...O-3f(–C-3f)		2.79 (199°)	3.07 (118°)
Ow1...O-1g		3.17	3.44
Ow2...O-1f(–C-1f)			2.79 (116°)
Ow3...O-3f(–C-3f)		2.81 (138°)	2.80 (139°)
Ow4...O-3f(–C-3f)		2.85 (102°)	
Ow5...O-4f(–C-4f)		3.24 (122°)	2.81 (126°)
Ow6...O-2g(–C-2g)		3.21 (92°)	3.21 (91°)
Ow7...O-3g(–C-3g)		2.74 (118°)	
Ow8...O-3g(–C-3g)		3.25 (143°)	3.28 (138°)

the hydration (interactions with water oxygens) along with geometrical details are listed in Table 1 and compared to the anhydrous neutron structure of sucrose [12]. Table 1 also lists the details of the sucrose hydration with respect to first hydration shell polar waters in the lectin crystal. The hydration is quite similar for the two molecules with minor changes in the firmness of the binding of the bridging water molecules and absence of possible hydration sites due to interactions with the lectin molecules.

3. Results and discussion

Analysis of the sucrose hydration from the MD simulations.—Radial hydration of acetal and hydroxyl solute oxygens. Radial pair distribution functions of the solute oxygens with respect to water oxygens are shown in Fig. 3 and the details are listed in Table 2. The pair distributions of the hydroxyl oxygens display typical hydrophilic hydrogen bonding behaviour [15,16]. The sharp first peak at 2.8 Å indicates a strong radial location of the hydrogen bonded nearest neighbour water molecules in the first hydration shell. The first minimum, at approximately 3.7 Å, indicates the outer limit of the first hydration shell. At this distance, the water density has decreased to a little more than half of the bulk water density. This indicates a strong radial water structuring around the hydroxyl oxygens, and substantial shielding effect between the first hydration shell water molecules and the surrounding bulk water molecules. In the centre of the first hydration shell water densities were calculated ranging between 2.09 (O-4f) and

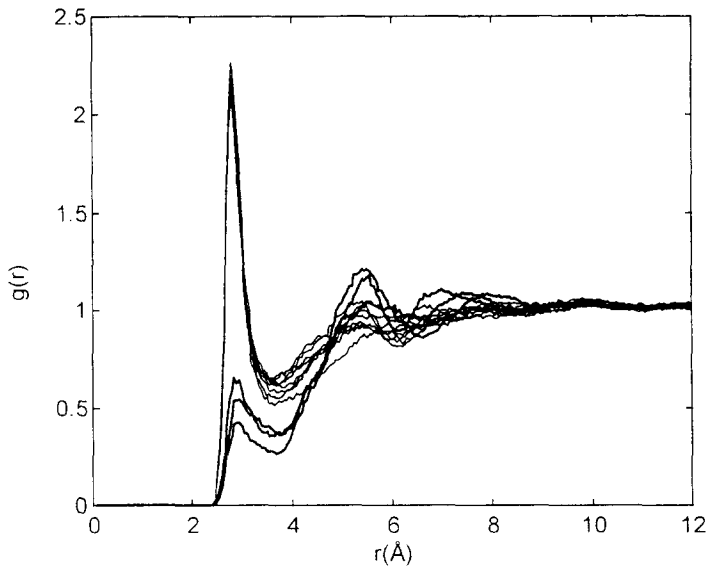

Fig. 3. Radial pair distribution functions $g(r)$ of water oxygens around solute oxygens. Distances (x-axis) are in Å.

2.27 (O-3g and O-6g) times the bulk water density. By integration of the radial pair distribution functions one can obtain the number of nearest neighbour water molecules in the first hydration shell around each solute atom. The hydroxyl oxygens were found to have between 3.9 (O-3f) and 4.4 (O-3g) nearest neighbours indicating saturated hydrogen bonding (1 donor and 2 acceptors) capacity and the existence of, to the solute,

Table 2
Characteristics of the radial water oxygen–solute oxygen distributions. The first hydration shell. The integrated hydration numbers have been obtained by integration between $r(0)$ and $r(\min)$ or between $r(0)$ and $r(3.5)$. Distances are in Å

Atom	Maximum		Minimum		Close neighbours	
	r	$g(r)$	r	$g(r)$	$I_0^{\min}$	$I_0^{3.5}$
O-1g	2.9	0.42	3.7	0.26	1.5	1.2
O-2g	2.8	2.20	3.7	0.55	4.6	4.0
O-3g	2.8	2.27	3.8	0.62	5.2	4.4
O-4g	2.8	2.18	3.7	0.58	4.7	4.1
O-5g	2.9	0.65	3.7	0.36	2.0	1.7
O-6g	2.8	2.27	3.7	0.64	5.0	4.3
0-1f	2.8	2.25	3.7	0.61	4.9	4.2
O-3f	2.8	2.09	3.7	0.51	4.3	3.9
O-4f	2.8	2.13	3.9	0.60	5.3	4.1
O-5f	3.0	0.54	3.8	0.36	2.2	1.6
O-6f	2.8	2.19	3.7	0.64	4.7	4.1
Σ		18.79			44.4	37.6

non-hydrogen bonded water molecules in the first hydration shell. Such 'oversaturated' hydration patterns have previously been found in the vicinity of carbonyl or hydroxyl oxygens in pure water [17], dipeptide solvation [13], carbohydrate solvation [18], and triglyceride solvation [16]. The radial pair distribution functions of the hydroxyl oxygen also show some long range structure with a peak at about 5.5 Å indicating the centre of the secondary hydration shell.

The radial pair distribution functions for the three acetal solute oxygens display significantly different hydration behaviour from those of the hydroxyl oxygens (see Fig. 3). The first peaks of these functions are perturbed and far from reaching the bulk density. As listed in Table 2, the geometries of the first hydration shell around these atoms are comparable to those of the hydroxyl oxygens with first peak at about 2.9 Å and first minimum around 3.7 Å, except that the water densities are much lower. We ascribe this difference mainly to the fact that the acetal oxygens are less exposed to the water than the hydroxyl oxygens due to the ring geometries and the proximity of other groups. The hydration numbers of the three acetal oxygens reveal a much lower hydration when compared to the hydroxyl oxygens, but also a significant difference between the glycosidic oxygen and the ring oxygens. While the two ring oxygens have hydration numbers of 1.6–1.7 the glycosidic oxygen is considerably less hydrated with only 1.2 nearest water molecules in the first hydration shell. This rather large difference for two identical types of atoms can only be ascribed to a limited water accessibility to the highly crowded glycosidic region of the sucrose solute.

Global solute hydration. The close proximity of the eight hydroxyl and three acetal oxygens results in a relatively large hydrodynamic size with many shared polar water molecules between different solute oxygens. The sum of all the closest neighbours, $I(0 \rightarrow 3.5$ Å) (see Table 2) results in a molecular hydration number of $h = 37.6$ water molecules in the first hydration shell (many of these water molecules are shared between different groups and count more than one). In order to investigate the hydration of sucrose we calculated the number of polar water molecules in its close surroundings (less than 3.5 Å from the solute oxygen) as a function of time. The result shown in Fig. 4a reveals a fluctuating time series with hydration numbers ranging between 15 and 35. The average hydration number is $h = 24.7$ polar water molecules per sucrose molecule. Using this type of definition, the first hydration shell around sucrose is rather large with almost 13 shared water molecules (37.6–24.7). The hydration number for sucrose of $h = 5.3$ can be deduced from the Stokes–Einstein relationship assuming spherical geometry of the solute [19]. A hydration number for sucrose of $h = 5$ was obtained [20] from the activity of water in dilute sucrose solutions when compared to the activity of pure water. A hydration number for sucrose of $h = 6.8$ was derived [21] from the *B*-viscosity and the apparent molar volume. Finally, twice the hydration number for sucrose, $h = 13.9$, was obtained from ultrasound measurements [22]. Such a discrepancy in experimental determination of the hydration number of sucrose is intriguing and points toward different definitions of hydration number. If instead of using the first hydration shell, we restrict the 'hydration criterion' to include only distances less than 2.8 Å (where the hydration of hydroxyl oxygens reaches maximum density), we obtain an average hydration number of $h = 7.0$ (see Fig. 4b). This is in line with the determination using the *B*-viscosity and apparent molar volume. The low experimental

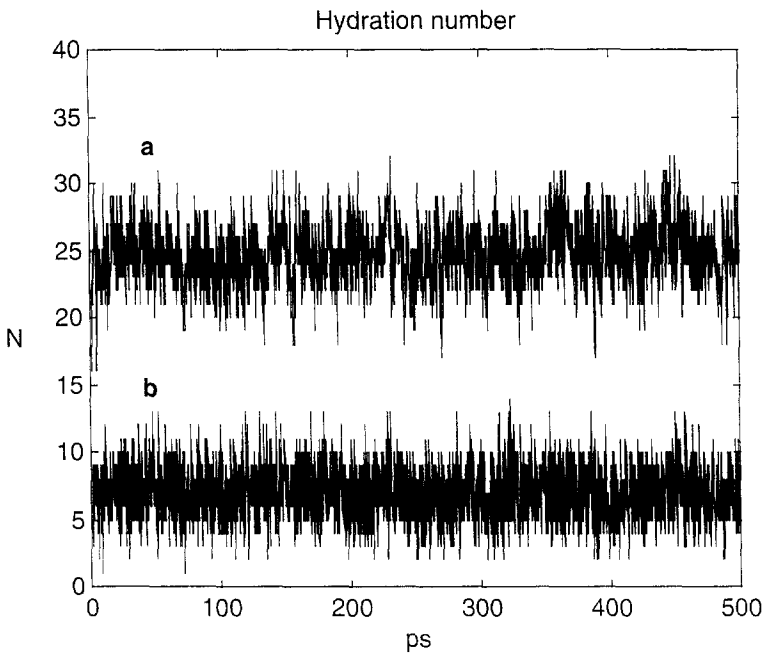

Fig. 4. (a) Time series monitoring the number of polar water molecules in the first hydration shell around the solute. Polar water molecules are defined as being closer than 3.5 Å to one of the solute oxygens. The average solvation number in the production trajectory is 24.7. (b) Time series monitoring the number of strongly polarized water molecules in the first hydration shell defined as being closer than 2.8 Å to one of the solute oxygens. The average solvation number in the production trajectory is 7.0.

hydration numbers for sucrose indicate that the firmly hydrogen bonded water molecules have more impact on the macroscopic properties than the theoretical shielding effect formed by the first hydration layer.

Orientational hydration of acetal and hydroxyl solute oxygens. Orientational distributions around the solute oxygen have been characterized. They complement the assessment of the orientational structuring characteristics of the closest water molecules. Some selected orientational distributions around solute oxygens are shown in Fig. 5. As in the case of the radial distributions, the orientational distributions of the hydroxyl oxygens are very similar and display typical hydrophilic solvation behaviour; this is exemplified in Fig. 5 by the orientational distribution around O-6g. The strong peak at $\cos\theta = -1.0$ indicates a typical hydrogen-bond-acceptor behaviour where one of the Ow–H bonds of the water molecule points directly toward the solute oxygen. The broad secondary peak between $\cos\theta = 0.0$ and $\cos\theta = 0.5$ is a consequence of the rigid and tetrahedral TIP3P water geometries with a contribution from accepting water oxygens. In contrast to the strong hydrophilic solvation character of the hydroxyl oxygens, the acetal oxygens display much weaker hydrogen bonding behaviour. The maximum probability of the angle between the water Ow–H bonds and the solute oxygen occurs at approximately $\cos\theta = -0.8$ and the orientational distributions are considerably less structured. The

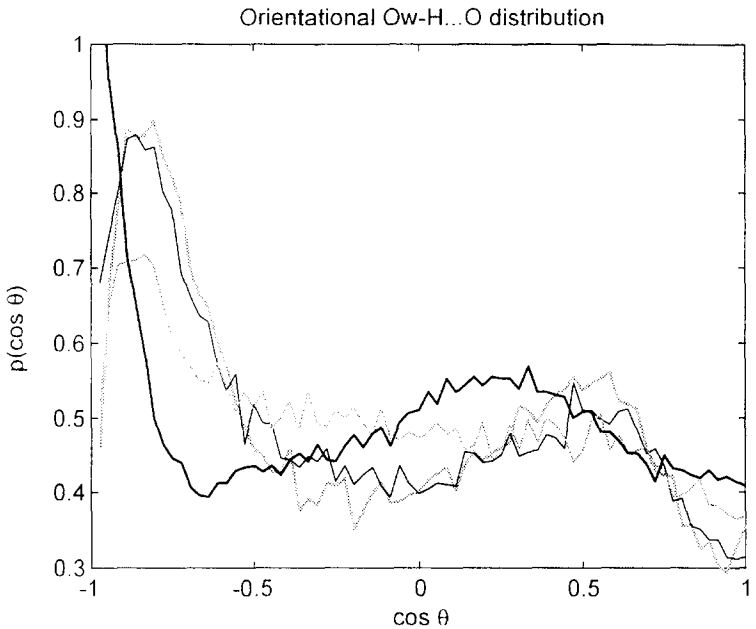

Fig. 5. Orientational Ow–H...O distribution functions $p(\cos\theta)$ of polar water molecules in the first hydration shell around solute defined by radii of 3.5 Å for the polar solute atoms. Typical hydroxyl oxygen solvation O-6f (thick black) compared to the solvation of the three ether oxygens: O-1g (thick gray), O-5g (thin black), and O-5f (thin gray).

reason for this deviation from a typical hydrophilic orientational behaviour has to be sought in local competition for the water molecules as well as differences in local dipole–dipole interactions. The glycosidic oxygen O-1g has a different radial hydration from the other two ether oxygens. Fig. 5 indicates that with respect to the orientational structure, the O-5f ring oxygen atom has a different hydration scheme. The orientational distribution of water molecules around O-5f is considerably flatter and thus less structured than the two other ether oxygens; this is ascribed to puckering phenomena (vide supra).

The orientational water structuring around the solute can also be described by orientational distribution functions around Cs–Os...Ow including only heavy atoms; this provides a means of comparison with the hydration in the sucrose–lectin structure. These orientational distribution functions are shown in Fig. 6 for all eight hydroxyl sucrose oxygens. In simple randomly distributed systems where no steric conflict is possible (no O–H bonds, etc.) one would observe a normal distribution about $\cos\theta = 0.0$. The maxima for these distributions occur around $\cos\theta = -0.36$; this is very close to the tetrahedral angle ($\cos\theta = -0.33$), indicating a tendency to incorporate the heavy atoms of the solute into the quasi-tetrahedral network of the water solvent with hydrogen bonding pointing toward the lone pair positions of the oxygens. The distributions decrease to zero around $\cos\theta = 0.5$; this is because inclusion in the first hydration shell is not allowed from behind, and certainly not in these ring systems. The smaller peaks at

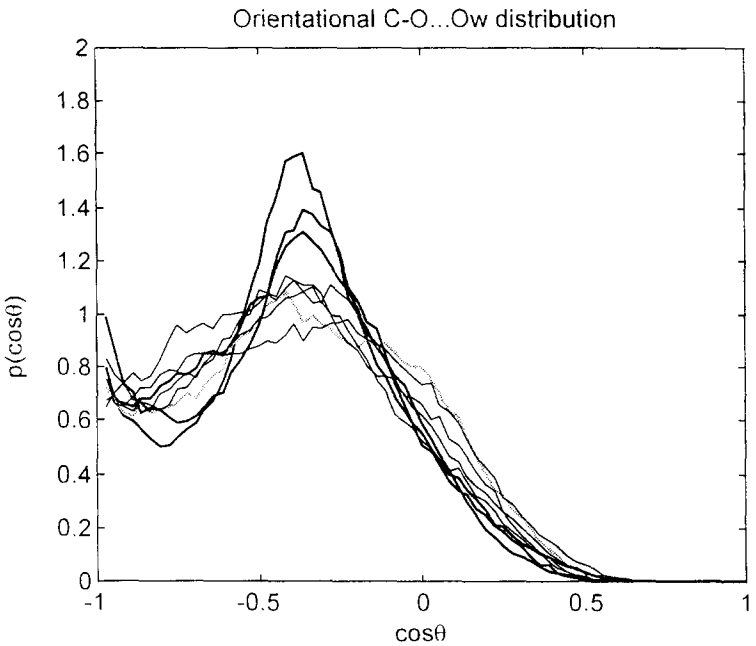

Fig. 6. Orientational C–O...Ow distribution functions p(cos θ) of polar water molecules in the first hydration shell around solute defined by radii of 3.5 Å for the polar solute atoms. The three pyranosyl secondary hydroxylic oxygens are marked with thick black line and the pyranosidic primary hydroxylic oxygen is marked with a thick gray line.

cos $\theta = -1.0$ are interesting, as such an arrangement is relatively improbable. It was found that part but not all of the increased probability at cos $\theta = -1.0$ arises from the outer layer of the first hydration shell, presumably due to the tetrahedral network. Finally, it is obvious from the relatively sharp peaks in Fig. 6 that the water structure around the three secondary hydroxyl groups on the pyranosyl ring in glucose (O-2g, O-3g, and O-4g) are much more structured, indicating a more perfect hydration of this relatively rigid part of the sucrose molecule. When comparing above orientational distributions with the static hydration geometries of the sucrose molecules in the lectin complex (Table 1), it is observed that the latter are all found within the main probabilistic peak from about cos $\theta = -0.2$ to about cos $\theta = -0.8$. Both extremes are found in cases with doubly hydrated solute oxygens (O-2g and O-3g) which encompass a more 'perfect' hydration geometry.

Residence times for polar water molecules around the sucrose solute. The fluctuations in the hydration numbers of sucrose shown in Fig. 4 are a reflection of the dynamic exchange of water molecules in the hydration shell. In order to investigate the static aspect of the hydration shell we calculated the maximal and average residence times for all water molecules in the first hydration shell (Fig. 7). The results listed in Table 3 reveal quite large differences in the maximal as well as average residence time for the polar water molecules. The polar water molecules around the acetal oxygens display significantly lower average residence times than those around the hydroxyl oxygens, and

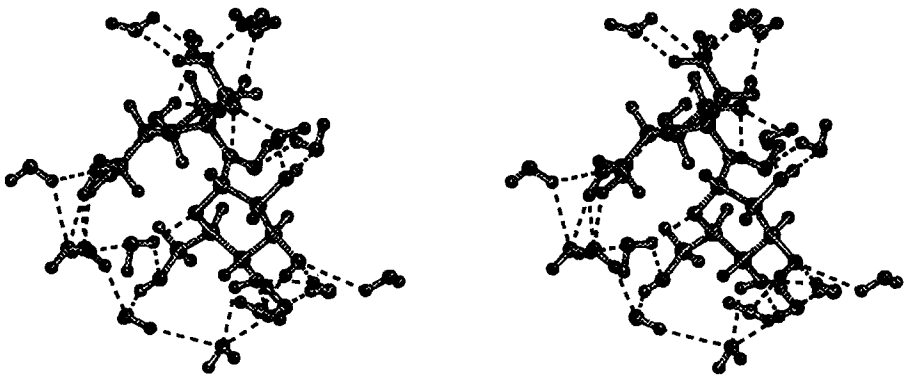

Fig. 7. Stereo view of the first hydration shell after 380 ps.

they are only hydrated on a 90% population level. In contrast, all the hydroxyl oxygens are hydrated on a 99–100% level. Equally interesting are the large differences in the average residence times for water molecules around the hydroxyl oxygens (Table 3). The primary hydroxyl oxygens exhibit similar behaviour, with average residence times for polar water molecules between 1.71 ps and 1.84 ps, whereas the secondary hydroxyl oxygens show average residence times between 1.19 (O-3g) and 2.35 ps (O-4g). In the pyranose ring the O-3g oxygen shows a significantly lesser tendency to preserve the water molecules, as indicated by an average residence time of 1.2 ps when compared to

Table 3
Residence times for polar water molecules around solute oxygens. DC indicates the distance criterion used and AC indicates if an angle criterion ($\cos\theta < -0.8$) has been used to accept hydrogen bonding. Times are in ps and distances are in Å. p is the probability of finding at least one water molecule meeting the DC and AC criteria

Atom	Criteria		Maximum		Average	
	DC	AC	#water	t	$\langle t \rangle$	p
O-1g	3.5	–	287	9.36	0.60	0.86
O-2g	3.5	–	205	13.66	2.21	0.99
O-3g	3.5	–	221	9.02	1.19	1.00
O-4g	3.5	–	319	15.02	2.35	1.00
O-5g	3.5	–	120	13.30	0.79	0.93
O-6g	3.5	–	284	17.08	1.80	1.00
O-1f	3.5	–	193	19.08	1.84	0.99
O-3f	3.5	–	288	30.10	2.25	0.99
O-4f	3.5	–	136	10.34	1.82	0.99
O-5f	3.5	–	103	11.66	0.60	0.90
O-6f	3.5	–	100	3.42	1.71	0.99
O-2g	3.0	–	324	2.98	0.23	0.97
O-2g	3.5	+	138	1.90	0.11	0.82
O-3f	3.0	–	288	4.88	0.25	0.97
O-3f	3.5	+	482	2.62	0.12	0.83

2.2 and 2.4 ps for the neighbouring groups: O-2g and O-4g, respectively. The water molecules around these oxygens are relatively fixed. This is consistent with the fact that the configurations of the hydroxyl groups O-4 and O-2 in pyranoses have proven to be essential in maintaining the overall compatibility of the carbohydrate with the three-dimensional hydrogen bonded network of water [22]. In the fructofuranosyl ring system we observe a relatively large difference between the water residence times of the secondary hydroxyl groups O-3f (2.3 ps) and the other hydroxyl oxygens (around 1.8 ps) as also indicated by the very large maximal residence time of 30 ps for water number 288. This may indicate that the O-3f hydroxyl group acts as a fixed point with respect to the water structure while the fructofuranosyl ring undergoes puckering dynamics.

Analysis of significant bridging water molecules. Modelling studies [2,23] and NMR studies [24,2,3] have recently converged to agree that interresidue hydrogen bonds in sucrose, as observed in the crystal structure [12], are not persistent in dilute water solutions. Perhaps more convincingly, two independent sucrose molecules have recently been co-crystallized, extensively hydrated, with a lentil lectin, and in both structures no interresidue hydrogen bonds are observed and both exhibited an interresidue bridging water molecule between O-1g and O-3f [4]. We have preliminarily reported that the situation where the sucrose molecule possesses a structure with a bridging water between O-2g and O-3f has a statistical significance of about 25% in the 0.5 ns MD trajectory analyzed here [2]. Sheng and van Halbeek [3] proposed the existence of a weak and at least transiently existing O-2g...O-1f interresidue hydrogen bond from NOESY experiments in supercooled solutions. From modelling studies Immel and Lichtenthaler [23] proposed the existence of a O-2g...Ow...O-1f bridging water which prevails with high significance and long life-time. To investigate the significance of the two possible types of interresidue bridging water molecules in our MD trajectory, we performed a series of calculations of shared water molecules between O-2g, O-3f, O-1f, and O-1g. The results of these calculations are summarized in Table 4. A shared water molecule in the first hydration shell between O-2g and O-3f occurs on a 41% basis. The maximum residence time observed was 9 ps, whereas the average residence time was 0.48 ps. If the hydration criteria are strengthened to include only firmly hydrogen-bonded water molecules with a Ow–H...Os angle less than $\cos\theta < -0.8$, we reduce the significance to 10% and the average residence time to 0.07 ps. In comparison, the direct interresidue hydrogen bond O-2g...O-1f occurs less than 4% of the time.

The situation with a shared water molecule in the first hydration shell between O-2g and O-1f occurs on a 66% basis and is thus even more populated than the O-2g...Ow...O-3f situation. The maximum residence time for the shared water between O-2g and O-1f was found to be similar to that of the O-2g...Ow...O-3f, whereas the average residence time was longer, namely 0.67 ps. Again, if we strengthen the hydration criteria we obtain an occupancy level of 26% and average residence time of 0.08 ps. We also investigated the possibility of a shared water molecule between the three solute oxygens O-2g, O-1f, and O-3f, and indeed such a situation was relatively highly populated: 21% (Fig. 8). However, we were not able to detect any statistical transition phenomena between the two bridging situations, and even though water number 287 was occurring with maximum residence 'habit' in both places it took place in quite different parts of the trajectory. The most resident bridging water molecule

Table 4
Residence characteristics for bridging waters in the pocket defined by the four solute oxygen atoms: O-2g, O-1f, O-3f, and O-1g. DC indicates the distance criterion used and AC indicates if an angle criterion $\cos\theta < -0.8$ has been used to accept hydrogen bonding. Times are in ps and distances are in Å. p is the probability of finding at least one water molecule meeting the hydrogen bonding criteria

Criteria					Maximum		Average	
O-2g	O-3f	O-1f	O-1g	AC	#water	t	$\langle t \rangle$	p
3.5	3.5	–	–	–	287	9.06	0.48	0.41
3.5	3.5	–	–	+	50	1.62	0.12	0.27
3.0	3.0	–	–	–	451	0.70	0.09	0.13
3.0	3.0	–	–	+	451	0.70	0.07	0.10
3.5	*3.5*	–	*3.5*	–	*287*	*9.02*	*0.43*	*0.39*
2.8	*3.1*	–	*3.5*	–	*290*	*0.30*	*0.05*	*0.05*
2.8	*2.8*	–	*3.2*	–	*290*	*0.18*	*0.03*	*0.01*
3.5	–	3.5	–	–	287	9.24	0.67	0.66
3.5	–	3.5	–	+	289	2.32	0.13	0.48
3.0	–	3.0	–	–	324	1.10	0.13	0.36
3.0	–	3.0	–	+	451	0.84	0.08	0.26
3.5	3.5	3.5	–	–	287	4.14	0.32	0.21
3.0	3.0	3.0	–	–	451	0.56	0.07	0.04

between O-2g and O-3f was found while χ_f is in the TG orientation from where a O-2g...Ow...O-1f bridging water situation is able to compete (or perhaps stabilize).

The influence of fructofuranosyl puckering upon the water structure. In the 0.5 ns trajectory which we analyzed, the northern and southern puckering wells are populated equally and 12 puckering transitions were observed [2]. It was observed that the solvent had a general broadening effect on the available conformational space. As observed in arabinofuranose (Cros et al., 1993), the northern conformation of the fructofuranosyl ring has all the ring hydrogens in axial positions which results in a small hydrophobic surface pointing toward the solvent. This is also reflected in the polarity of the molecule. An evaluation of MM3 dipole moments in vacuo using MM3 [25] results in approximately 5 D and 4 D for the northern (X-ray conformation) and the southern well, respectively.

In the previous study [2] we were not able to establish any geometrical correlation with the fructofuranosyl puckering. We, therefore, conducted an investigation of differences in the water structure around the fructose residue. In the northern conformation the 'all axial hydrogen' geometry of the fructose residue will express a sufficiently large hydrophobic surface to induce changes in the local water structure. To this end we calculated pair distribution functions for all the heavy atoms concerned with respect to the solvent oxygens in the northern and in the southern conformation; only very minor differences in the radial hydration were revealed. Then, orientational distributions of the first hydration shell waters with respect to the same solute heavy atoms were calculated. It has been established that when water is in contact with large hydrophobic surfaces it

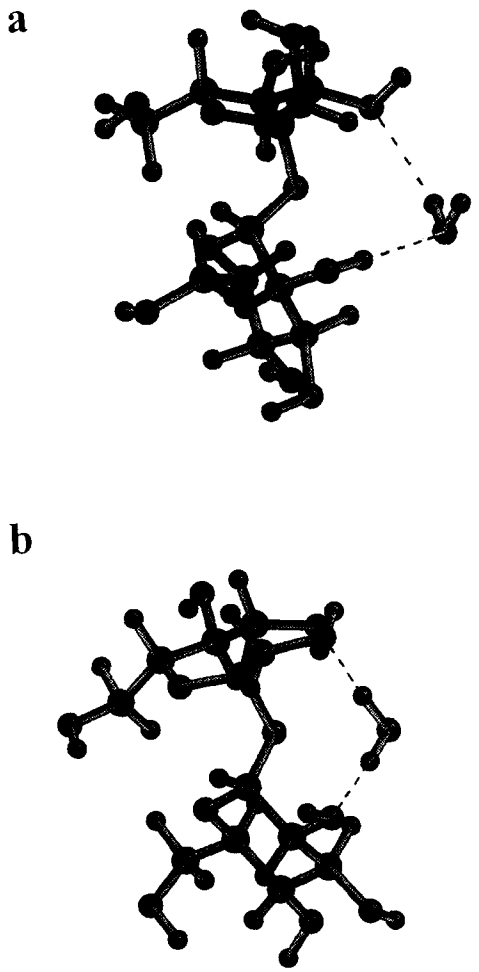

Fig. 8. Snapshot displaying the position of the bridging water molecule. (a) The O-2g...Ow...O-3f bridge; (b) the O-2g...W...O-1f bridge.

minimizes the overall loss of hydrogen bonds by sacrificing a hydrogen bond by pointing it directly towards the hydrophobic surface [26]. Such a dramatic effect is not observed when the fructofuranosyl ring is in the 'hydrophobic' northern conformation. However, the orientational distribution around C-3f (Fig. 9) which displayed large residence times clearly shows that a perturbation is present when the fructose residue resides in the northern conformation. In the southern conformation the orientational distribution displays a normal 'single point' non-polar character [16,27] with a peak at $\cos\theta = 1.0$ indicating a tendency of one of the hydrogen atoms of the water molecule to point directly away from the non polar group. The peak around $\cos\theta = -0.5$ is a geometrical consequence of the tetrahedral TIP3P water geometry and the deep minimum at $\cos\theta = -1.0$ indicates that there is very little probability of finding a hydrogen

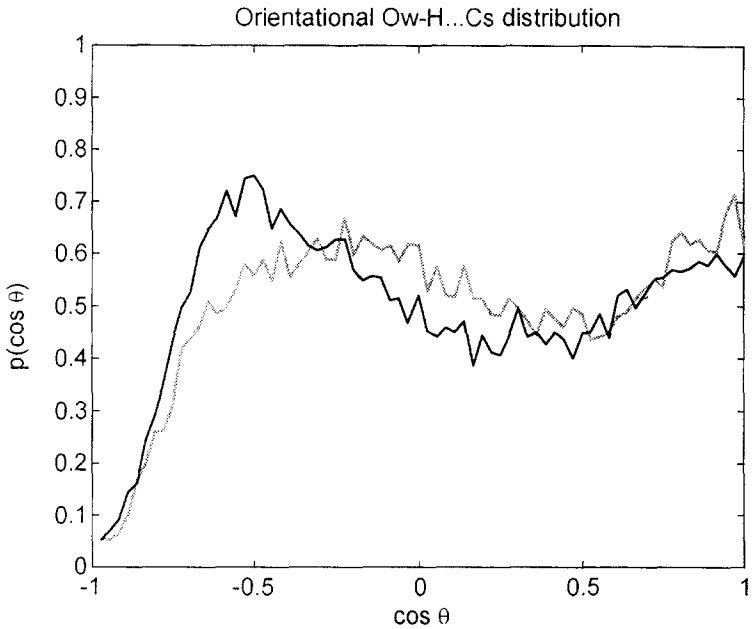

Fig. 9. Orientational hydration distribution around C-3f when the fructofuranosyl ring are in the northern (thick gray) and southern (thick black) conformation.

atom pointing directly toward the solute carbon. The perturbation (flatter distribution) of the orientational hydration around O-3f indicates a less ordered arrangement of the water molecules when in the northern conformation, but the probability of sacrificing a hydrogen bond by pointing directly toward the solute carbon C-3f has not increased. This demonstrates a very delicate balance between the most favoured in vacuo structure of the fructofuranosyl ring and the most favoured water solution structure of the fructofuranosyl ring.

Comparison with the hydration of sucrose complexed to a protein. From Table 1 it is noteworthy that the two sucrose molecules, designated as L1 and L2, are quite similar in terms of geometry, indicating a similar type of hydration. Comparison with the neutron structure of anhydrous sucrose reveals some significant changes. While the primary hydroxyl group of glucose (ω_g) and the glycosidic linkage parameters (Φ, Ψ, and θ) are quite similar, indicating a firmly bound glucose moiety almost like in the pure sucrose crystal, the fructofuranosyl residue displays significant changes. Both the primary hydroxyl groups of fructose (ω_f and χ_f) have adopted conformations (GT and GG, respectively) which differ from those of the crystalline conformation (GG and TG, respectively); this is in good agreement with the preferred rotamers of sucrose in aqueous solution [2]. These results along with a visual inspection of the sucrose lentil lectin complex indicate a loosely bound fluctofuranosyl moiety existing as if in aqueous solution. The average puckering amplitude of the fructofuranosyl ring in the solution trajectory was 0.340 compared to the 0.353 in the crystal structure and 0.46 in the lectin–sucrose complex. The high puckering amplitude of the fructofuranosyl ring in the

crystalline complex may indicate some induced strain; it may also result from experimental uncertainties.

An interesting difference in the geometric details is the absence in L1 and L2 of the two interresidue hydrogen bonds, as indicated by the non-bonded distances: O-2g...O-1f and O-5g...O-6f. Moreover, a bridging water molecule between O-2g and O3-f is present in both L1 and L2 which leads to a slightly shorter O-2g...O-3f distance.

There exists a high degree of similarity between the sucrose hydration derived from the 0.5 ns MD trajectory and the sucrose hydration found in the lectin complex. In the first hydration shell of L1 (Table 1) we find 7 water molecules of which 5 are strongly hydrogen bonded. In the first hydration shell of L2 we find 6 water molecules of which 4 are strongly hydrogen bonded. In none of the structures are O-4g, O-6g, O-1f, and O-6f hydrated due to interactions with the lectin. In L1, O-2g and O-3g are doubly hydrated and C-3f triply hydrated whereas in L2 only O-2g and O-3f are doubly hydrated. Due to the interaction competition with the protein it is difficult to compare such hydration numbers. Nevertheless, when considering the hydration features of the non-bound fructofuranosyl moiety, it appears that the long residence time in the MD trajectory coincides with the strong hydration in the sucrose lectin complex (compare O-3f which is strongly hydrated with O-1f, O-4f, and O-5f). The hydration distances and angles (Table 1) are located in highly populated areas of the radial pair distribution functions (Fig. 3 and Table 2) and orientational C–O...Ow distribution functions (Fig. 6).

The bridging water between O-2g and O-3f found in both L1 and L2 can perhaps be enforced by protein interactions with O-1f making the slightly higher populated O-2g...Ow...O-1f situation impossible. However, the O-2g...Ow...O-3f bridge is found populated 27% in the MD trajectory (Table 4) and as such must be assumed to be a possible candidate for a global minimum structure. The exact radial bridging geometries with respect to O-2g, O-3f, and also O-1g found in L1 and L2 are found in the dynamic trajectory to be populated between 1 and 5% (Table 4, italics), underlining the importance of such a geometrical arrangement.

4. Conclusions

There is a striking convergence between the results derived from the MD simulation and those observed in the crystal structure of the complex with the protein, with respect to the occurrence of the water-mediated hydrogen bond bridge between O-2g and O-3f. Such a scheme is likely to represent a significant structural feature of the conformational behaviour of hydrated sucrose that may persist up to the high concentration stage. It may therefore have significant implications on the complex crystallization of sucrose, vis-à-vis the extent of supersaturation which persists before nucleation takes place. The removal of the bridging water molecule is a requirement for the intramolecular hydrogen bond between O-2g and O-1f to occur. Such a transition requires a rotation of 120° of the primary hydroxyl group about χ_f. It should nevertheless be emphasized that the transition toward the crystalline conformation just implies small adjustments about the

glycosidic torsion angles, Φ and Ψ. Presumably, this will be accompanied by the formation of the second intramolecular hydrogen bond between O-6f and O-5g.

Acknowledgements

As parts of this study have been done in France and parts in Denmark, both the French program Conception MacroMolecules Assistée par Ordinateur (Organibio) and the Danish Food Research Centre for Advanced Studies (LMC) are gratefully acknowledged. S.P. is a research fellow of Institut National de la Recherche Agronomique.

References

[1] S. Pérez, *Sucrose Properties and Applications*, M. Mathlouthi and P.H. Reiser (Eds.), Chapman and Hall, London, 1994, pp 11–30.
[2] S.B. Engelsen, C. Hervé du Penhoat, and S. Pérez, *J. Phys. Chem.*, 99 (1995) 13334–13351.
[3] S. Sheng and H. van Halbeek, *Biochem. Biophys. Res. Commun.*, 215 (1995) 504–510.
[4] F. Casset, T. Hamelryck, R. Loris, J.-R. Brisson, C. Tellier, M.-H. Dao-Thi, L. Wyns, F. Poortmans, S. Pérez, and A. Imberty, *J. Biol. Chem.*, 270 (1995) 25619–25628.
[5] IUPAC-IUB, Commission on Biochemical Nomenclature, *Arch. Biochem. Biophys.*, 145 (1971) 405–421; *J. Mol. Biol.*, 52 (1970) 1–17.
[6] D. Cremer and J.A. Pople, *J. Am. Chem. Soc.*, 97 (1975) 1354–1358.
[7] S.N. Ha, A. Giammona, M. Field, and J.W. Brady, *Carbohydr. Res.*, 180 (1988) 207–221.
[8] B. Brooks, R. Bruccoleri, B. Olafson, D. States, S. Swaminathan, and M. Karplus, *J. Comp. Chem.*, 4 (1983) 187–217.
[9] W.L. Jorgensen, *J. Am. Chem. Soc.*, 103(2) (1981) 335–340.
[10] L. Verlet, *Phys. Rev.*, 159 (1967) 98–103.
[11] W.F. Van Gunsteren and H.J.C. Berendsen, *Molec. Phys.*, 34 (1977) 1311–1327.
[12] G.M. Brown and H.A. Levy, *Acta Crystallogr., Sect. B.*, 29 (1972) 790–797.
[13] P.J. Rossky and M. Karplus, *J. Am. Chem. Soc.*, 101 (1977) 1913–1937.
[14] F.C. Bernstein, T.F. Koetzle, G.J.B. Williams, E.F. Meyer, M.D. Brice, J.R. Rodgers, O. Kennard, T. Shimanouchi, and M. Tasumi, *J. Mol. Biol.*, 112 (1977) 535–542.
[15] J.W. Brady, *J. Am. Chem. Soc.*, 111 (1989) 5155–5165.
[16] S.B. Engelsen, J.W. Brady, and J.W. Sherbon, *J. Agric. Food Chem.*, 42 (1994) 2099–2107.
[17] A. Rahman and F.H. Stillinger, *J. Phys. Chem.*, 44 (1971) 3336.
[18] J.W. Brady and R.K. Schmidt, *J. Phys. Chem.*, 97 (1993) 958–966.
[19] M. Mathlouthi and J. Génotelle, in: Mathlouthi and Reiser (Eds.), *Sucrose*, Blackie Academic and Professional, 1994, pp 127–154.
[20] E.I. Akhumov, *Russian J. Phys. Chem.*, 55 (1981) 837–839.
[21] M.-O. Portman and G. Birch, *J. Sci. Food Agric.*, 69 (1995) 275–281.
[22] S.A. Galema and H. Høiland, *J. Phys. Chem.*, 95 (1991) 5321–5326.
[23] S. Immel and F.W. Lichtenthaler, *Liebigs Ann.*, (1995) 1925–1937.
[24] C. Hervé du Penhoat, A. Imberty, N. Roques, V. Michon, J. Mentech, G. Descotes, and S. Pérez, *J. Am. Chem. Soc.*, 113 (1991) 3720–3727.
[25] N.L. Allinger, M. Rahman, and J.-H. Lii, *J. Am. Chem. Soc.*, 112 (1990) 8293–8307.
[26] C.Y. Lee, J.A. McCammon, and P.J. Rossky, *J. Chem. Phys.*, 80 (1984) 4448–4455.
[27] J.W. Brady and R.K. Schmidt, *J. Phys. Chem.*, 97 (1993) 958–966.